Infection, Genetics and Evolution 67 (2019) 88–100

Contents lists available at ScienceDirect

Infection, Genetics and Evolution

journal homepage: www.elsevier.com/locate/meegid

Research paper

Microarray analysis of lncRNA expression in rabies virus infected human neuroblastoma cells

Senlin Ji[a], Mengyan Zhu[a], Junyan Zhang[a], Yuchen Cai[a], Xiaofeng Zhai[a], Dong Wang[d], Gairu Li[a], Shuo Su[a,*], Jiyong Zhou[a,b,c,**]

[a] MOE Joint International Research Laboratory of Animal Health and Food Safety, Engineering Laboratory of Animal Immunity of Jiangsu Province, College of Veterinary Medicine, Nanjing Agricultural University, Nanjing, China
[b] Key Laboratory of Animal Virology of Ministry of Agriculture, Zhejiang University, Hangzhou 310058, China
[c] Collaborative Innovation Center and State Key Laboratory for Diagnosis and Treatment of Infectious Diseases, First Affiliated Hospital, Zhejiang University, Hangzhou 310003, China
[d] China Institute of Veterina Drug Control, China

ARTICLE INFO

Keywords:
Rabies virus
Long noncoding RNAs
Microarray
Mechanism
Host

ABSTRACT

Rabies, caused by the rabies virus (RABV), is the oldest known zoonotic infectious disease. Although the molecular mechanisms of RABV pathogenesis have been investigated extensively, the interactions between host and RABV are not clearly understood. It is now known that long non-coding RNAs (lncRNAs) participate in various physiological and pathological processes, but their possible roles in the host response to RABV infection remain to be elucidated. To better understand the pathogenesis of RABV, RNAs from RABV-infected and uninfected human neuroblastoma cells (SK-N-SH) were analyzed using human lncRNA microarrays. We identified 896 lncRNAs and 579 mRNAs that were differentially expressed after infection, indicating a potential role for lncRNAs in the immune response to RABV. Differentially expressed RNAs were examined using Gene Ontology (GO) analysis and were tentatively assigned to biological pathways using the Kyoto Encyclopedia of Genes and Genomes (KEGG). A lncRNA-mRNA-transcription factor co-expression network was constructed to relate lncRNAs to regulatory factors and pathways that may be important in virus-host interactions. The network analysis suggests that E2F4, TAF7 and several lncRNAs function as transcriptional regulators in various signaling pathways. This study is the first global analysis of lncRNA and mRNA co-expression during RABV infection, provides deeper insight into the mechanism of RABV pathogenesis, and reveals promising candidate for future investigation.

1. Introduction

Mammalian cells contain large numbers of proteins that are encoded by a relatively small fraction of the genome. Although the functions of the remaining DNA sequences have been the subject of considerable speculation and research, high-throughput RNA sequencing and microarray technology have revealed that 70%–90% of the mammalian genome is transcribed to produce numerous noncoding RNAs (Djebali et al., 2012; Derrien et al., 2012) including long noncoding RNAs (lncRNAs), which contain 200 or more nucleotides (Derrien et al., 2012). Accumulating evidence suggests that lncRNAs participate in cell growth (Huang et al., 2014), development (Fatica and Bozzoni, 2014; Sauvageau et al., 2013), differentiation (Kretz et al., 2013; Wang et al., 2014), autophagy (Wang et al., 2015; Xiong et al., 2017) and apoptosis (Lu et al., 2013; Wu et al., 2014), through their ability to regulate gene expression at the transcriptional, post-transcriptional, and epigenetic levels (Lee, 2012). lncRNAs have also been implicated in diverse diseases and the immune response (Wang et al., 2016; Chen and Yan, 2013; Wu et al., 2017; Li and Rana, 2014), and disordered expression of lncRNAs is associated with infection by pathogens. For example, lncRNA nuclear enriched abundant transcript 1 (NEAT1) is expressed at high levels in response to infection by influenza virus (IAV) (Imamura et al., 2014), human immunodeficiency virus (HIV) (Zhang et al., 2013a), herpes simplex virus (HSV) (Wang et al., 2017a), dengue virus (Pandey et al., 2017), hantavirus (Ma et al., 2017), and other viral pathogens. Yang et al. reported the differential

* Corresponding author.
** Corresponding author at: MOE Joint International Research Laboratory of Animal Health and Food Safety, Engineering Laboratory of Animal Immunity of Jiangsu Province, College of Veterinary Medicine, Nanjing Agricultural University, Nanjing, China.
E-mail addresses: shuosu@njau.edu.cn (S. Su), jyzhou@zju.edu.cn (J. Zhou).

https://doi.org/10.1016/j.meegid.2018.10.027
Received 24 July 2018; Received in revised form 30 October 2018; Accepted 31 October 2018
Available online 02 November 2018

expression of thousands of lncRNAs in human macrophages after infection by *Mycobacterium tuberculosis*, and two lncRNAs were identified as novel candidate diagnostic markers for tuberculosis (Yang et al., 2016). Microarrays have been used to examine lncRNA expression profiles in mouse brains following infection by Japanese encephalitis virus (JEV) (Li et al., 2017). Differentially expressed lncRNAs in human neural progenitor cells (hNPCs) have been detected after Zika virus (ZIKV) infection, and may be involved in the microcephaly and Guillain-Barré syndrome described in some patients (Hu et al., 2017). These discoveries suggest that lncRNAs may be involved in host defenses against pathogenic microorganisms or may contribute to pathogenesis.

Rabies, the oldest known zoonotic infectious disease, causes neurological encephalitis and death (Fu, 1997). The World Health Organization estimates that > 50,000 victims succumb to the disease each year (Welburn et al., 2015). Although many rabies prevention and control strategies have been implemented (Tan et al., 2017), rabies remains a serious threat to human health, especially in Asia and Africa. The causative agent of rabies is the rabies virus (RABV), a member of the *Lyssavirus* genus in the *Rhabdoviridae* family. While both gene and protein expression have been examined in the host response to RABV, little is known about the role of lncRNAs during infection. To develop effective antiviral drugs and refine methods for the early detection of disease, it will be necessary to understand the pathogenic mechanisms of RABV infection in much more detail.

The molecular mechanisms of RABV infection are largely unclear, and investigations into the potential roles played by lncRNAs in rabies have been limited to NEAT1, a lncRNA that is highly expressed in mouse brain during RABV and Japanese encephalitis virus infection (Saha et al., 1991-1995). In this study, we examined lncRNA and mRNA expression profiles and compared expression patterns in RABV-infected and mock-infected human neuroblastoma cells. We identified 896 lncRNAs and 579 mRNAs that were differentially expressed after RABV infection. Potential biological functions of the differentially expressed lncRNA were explored using Gene Ontology (GO) analysis and Kyoto Encyclopedia of Genes and Genomes (KEGG) pathway analysis. Several strategies were used to explore possible 'cis' and 'trans' regulatory relationships between lncRNAs and target genes. A TF-lncRNA-gene network, generated using Cytoscape, suggests that the differentially expressed lncRNAs participate in the regulation of the immune response to RABV, and reveals potential targets for the diagnosis and treatment of rabies.

2. Materials and methods

2.1. Cell culture and viruses

The human neuroblastoma cell line SK-N-SH was purchased from ATCC (stock number HTB-11). Cells were cultured at 37 °C with 5% CO_2 in Eagle's Minimum Essential Medium (EMEM) supplemented with 10% fetal bovine serum (FBS) (Gibco/Invitrogen, Carlsbad, CA, USA). All media were supplemented with penicillin (100 U/mL) and streptomycin (100 g/mL). RABV strain CVS-11 was stored in our laboratory. During the experiment, SK-N-SH cells were infected with RABV at the indicated multiplicity of infection (MOI).

2.2. Determination of viral titers

Viral titers were determined by observing infected cells under a fluorescence microscope and calculating the 50% tissue culture infectious dose ($TCID_{50}$) using the Reed-Muench method (Zhang et al., 2013b). Briefly, cells were cultivated in 96-well culture plates (Corning, 3596) and then inoculated with 10-fold serial dilutions of virus. Infected cultures were maintained at 37 °C in 5% CO_2 for 48 h. After culture supernatants were removed, the cells were fixed in 100 mL cold acetone-methanol (1/1) at −20 °C for 30 min, and then allowed to air dry. The fixed cells were then incubated overnight with a monoclonal antibody against the RABV N protein at 4 °C. After 5 washes with phosphate-buffered saline (PBS), the cells were incubated with fluorescein isothiocyanate (FITC)-conjugated goat anti-mouse secondary antibody (Santa Cruz Biotechnology, Santa Cruz, Dallas, TX, USA) for 1 h at 37 °C. Cells were washed 4 times with PBS-Tween 20, and then virus titers were determined according to the presence of fluorescent staining using a fluorescence microscope (Nikon).

2.3. Cell collection, total RNA extraction, and quality control

Cells at 70 to 80% confluency in 6-well plates were rinsed twice with PBS, followed by the addition of diluted RABV (MOI = 1). After incubation for 1 h at 37 °C, the supernatant was discarded. The cells were then washed twice with PBS, and complete medium was added. After 24 h, infected cells were harvested and lysed in 1 mL of TRIzol reagent (Invitrogen). Total cellular RNA was isolated from the cells following the TRIzol manufacturer's protocol. A NanoDrop 2000 spectrophotometer (Thermo Scientific, Wilmington, DE, United States) and an Agilent 2100 (Agilent Technologies, California, United States) were used to determine RNA yield. RNA was subjected to agarose gel electrophoresis and ethidium bromide staining to evaluate RNA integrity. Only samples with OD_{260}/OD_{280} ratios between 1.8 and 2.1, and OD_{260}/OD_{230} ratios > 1.8, were acceptable. Samples were also required to be free of genomic DNA contamination and have a 28S/18S band intensity ratio > 2.0, as determined by staining after electrophoresis.

2.4. lncRNA and mRNA microarray expression profiling

Total RNA was labeled using the mRNA Complete Labeling and Hyb Kit (Agilent Technologies) and hybridized to the Agilent Human lncRNA 4*180 K Microarray (ID: 076500, Agilent Technologies). The microarray contains 32,776 probes for human mRNA and 78,243 probes for human lncRNAs, which are derived from authoritative sources including RefSeq (www.ncbi.nlm.nih.gov/refseq), Ensemble, genebank (www.ncbi.nlm.nih.gov/genbank) and the LNCipedia (https://lncipedia.org/). NONCODE (http://www.noncode.org/). After hybridization and washing, processed slides were scanned with the Agilent G2505C microarray scanner (Agilent Technologies). Raw data were extracted using Feature Extraction (version 10.7.1.1; Agilent Technologies). Quantile normalization and subsequent data processing were conducted using Genespring (version 12.0; Agilent Technologies) at the OE Biotechnology Company in Shanghai, People's Republic of China. The whole microarray datasets are available on NCBI GEO database, and GEO accession number is GSE119636.

2.5. Identification and clustering of differentially expressed lncRNAs and mRNAs

To identify differentially expressed lncRNAs and mRNAs, raw array data were normalized using GeneSpring (version 12.5) and then compared (infected vs. uninfected) using an unpaired *t*-test. According to previous report, RNAs were considered as differentially expressed if fold-change was ≥1.5 and differences between expression levels were statistically significant at $P \leq .05$(Sun et al., 2017). Differentially expressed lncRNAs and mRNAs were analyzed using Cluster 3.0 (Luo et al., 2015). Multiple test correction is implemented to reduce false positive or false discovery rates. The results were visualized using TreeView (http://taxonomy.zoology.gla.ac.uk/rod/treeview.html).

2.6. Gene ontology and KEGG pathway analyses of differentially expressed mRNAs

The gene ontology (GO) (www.geneontology.org) and Kyoto Encyclopedia of Genes and Genomes (KEGG) (http://www.genome.ad.jp/kegg/) databases were used to investigate potential biological functions and signaling pathways affected by differentially expressed

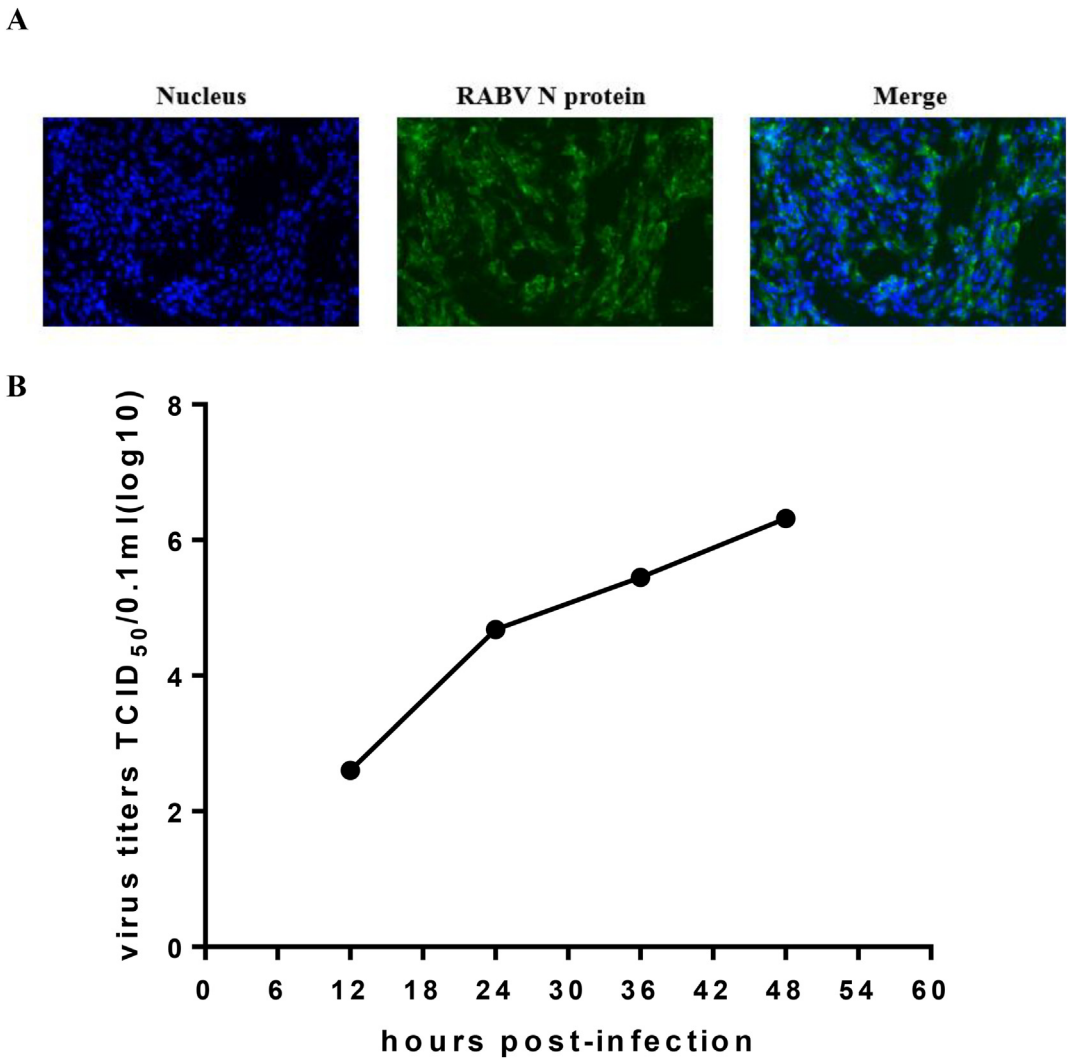

Fig. 1. RABV-infection of SK-N-SH cells. (A) Identification of RABV-infected SK-N-SH cells by IFA using a monoclonal antibody to recognize RABV N. (B) RABV infection kinetics in SK-N-SH cells. SK-N-SH cells were infected with RABV at a MOI of 1 and were collected at the indicated time points after infection for the determination of virus titers by TCID50 assays. Mean titers and standard deviations were calculated from three independent experiments.

mRNAs. Associations with *P*-values < .05 were considered to be statistically significant.

2.7. lncRNA-mRNA co-expression analysis and prediction of lncRNA function

To further explore the interactions between the differentially mRNAs and differentially expressed lncRNAs, the correlation of expressions between lncRNA and mRNA was calculated. For each lncRNA, we calculate the Pearson Correlation coefficient (https://libguides.library.kent.edu/SPSS/PearsonCorr) of its expression value with expression value of each mRNAs. The purpose of Pearson correlation here is to screen out mRNAs that are significantly co-expressed with lncRNA, and predict the function of this lncRNA. Each sample (6 samples) is treated as a separate data point. This calculation can comprehensively consider the expression relationship between lncRNA and mRNA in all samples of the experimental group and the control group. In this analysis, a correlation coefficient < 0.7 represented a negative correlation, and a value > 0.7 represented a positive correlation (Guttman et al., 2009). The correlation was considered significant for *P* values < .05. GO term and KEGG pathway enrichment analyses were performed for genes that were co-expressed with the differentially expressed lncRNAs, using cluster Profiler 3.0.1 in R (available at http://www.bioconductor.org/packages/release/bioc/html/clusterProfiler.html). We used the hypergeometric cumulative distribution function to calculate the enrichment of functional terms in the annotations associated with the co-expressed mRNAs. The False Discovery rate was calculated using a standard method (Storey, 2002). The enriched functional terms were used to predict functions for the lncRNAs.

2.8. Cis-regulation of lncRNAs

Many lncRNAs regulate their own transcription, as well as that of nearby genes, by recruiting remodeling factors to local chromatin (Guenzl and Barlow, 2012). We identified regions that are potentially subject to this type of cis-regulation using the following criteria: for each lncRNA, we classified mRNAs as “cis-regulated” when: (1) the mRNAs are encoded within 100 kbp upstream or downstream of a given lncRNA, (2) the Pearson correlation for lncRNA-mRNA expression is significant (*P*-value of correlation ≤ 0.05).

2.9. Correlation analysis between lncRNAs and transcription factors

After identifying mRNAs that were co-expressed with lncRNAs, we examined the co-expressed mRNAs to determine if they were known chromatin regulators or transcription factors (TFs), and then used the

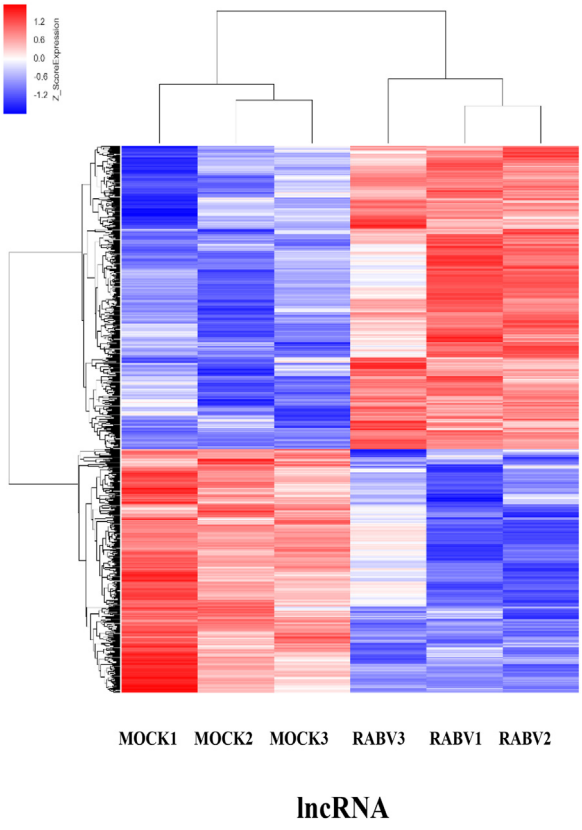

Fig. 2. Expression of lncRNAs in RABV-infected and mock-infected SK-N-SH cells. Heat map showing clustered expression profiles for differentially expressed LncRNAs. All expression values represent combined results obtained from three microarrays. Blue represents down-regulated genes and red represents up-regulated genes. (For interpretation of the references to colour in this figure legend, the reader is referred to the web version of this article.)

Encyclopedia of DNA Elements (ENCODE; www.encodeproject.org) to identify other genes whose expression might be controlled by the lncRNAs. Next, we analyzed our microarray data to determine whether the mRNAs encoding these genes were likely to be trans-regulated by the lncRNA of interest. Any previously identified co-expressed mRNAs were excluded from the analysis. The significance of a potential association was assessed using the hypergeometric cumulative distribution function. Significant lncRNA-TF-mRNA associations were used to construct a regulatory network, which was visualized with Cytoscape 3.3.0 (available at http://www.cytoscape.org/). If a gene is a target for a given TF, and the TF is co-expressed with a lncRNA, we hypothesize that the lncRNA is functioning as a trans-regulator for the gene (Gendrel and Heard, 2014).

2.10. Quantitative reverse transcription–polymerase chain reaction(qRT-PCR)

Total RNA was extracted using TRIzol reagent (Invitrogen). RT-PCR primers were designed based on the lncRNA sequences obtained from the Ensemble, LNCipedia and NCBI databases. The primers were synthesized and purified at Sangon Biotech (Shanghai, China). The RT reactions were performed using a cDNA synthesis kit (Thermo Scientific, Wilmington, DE, United States). Real-time PCR was performed using the Roche LightCycler® 480. The qPCR cycle was 98 °C for 2 min, followed by 45 cycles at 95 °C for 15 s and 60 °C for 30 s. A final melting curve analysis (60–95 °C) was included. The lncRNA PCR results were quantified using the $2^{-\Delta\Delta ct}$ method, normalized to GAPDH. The data represent the means of three independent experiments.

2.11. Statistical analysis

All results are expressed as means ± SEM. Statistical analysis was performed using GraphPad Prism 6 (GraphPad Software, San Diego, CA, USA). Differences were analyzed for statistical significance using a two-sided unpaired *t*-test for two groups or multiple comparison one-way of variance (ANOVA) for more than two groups (Bonferroni's multiple comparison test, $P < .05$).

3. Results

3.1. Proliferation of RABV strain CVS-11 in SK-N-SH cells

To determine the kinetics of RABV propagation in the human neuroblastoma cell line SK-N-SH, virus titers were measured and infection effects were examined at different time points after infection. Cells were infected at a MOI of 1 and then monitored at 12, 24, 36 and 48 h post-infection (hpi) using indirect immunofluorescence assays (IFAs). SK-N-SH cells infected by RABV were stained using a monoclonal antibody against the RABV N protein. As shown in Fig. 1A, the majority of cells were RABV-positive at 24 hpi. Relying on the Reed-Muench method, we

Table 1
The top 20 upregulated lncRNA between RABV infected group and the Mock group.

Rank	Target ID	Database	Fold change	Regulatio n	Chromosom al location
1	NONHSAT132573	NONCODE	23.238184	up	chr9
2	NONHSAT078622	NONCODE	13.416413	up	chr20
3	NONHSAT029216	NONCODE	8.765436	up	chr12
4	NONHSAT099045	NONCODE	8.75728	up	chr4
5	ENST00000438538	Ensemble	7.3308783	up	chr7
6	NONHSAT054767	NONCODE	6.872569	up	chr17
7	NONHSAT060898	NONCODE	6.0850997	up	chr19
8	NONHSAT106312	NONCODE	5.0581746	up	chr6
9	NONHSAT087325	NONCODE	3.7543898	up	chr22
10	NONHSAT092812	NONCODE	3.6754699	up	chr3
11	ENST00000595404	Ensemble	3.5006924	up	chr19
12	NONHSAT081892	NONCODE	3.3876865	up	chr21
13	NONHSAT122024	NONCODE	3.3634706	up	chr7
14	NONHSAT093065	NONCODE	3.2995589	up	chr3
15	NONHSAT030858	NONCODE	3.2606556	up	chr12
16	NONHSAT130225	NONCODE	3.2210333	up	chr9
17	NONHSAT116255	NONCODE	3.1240776	up	chr6
18	NONHSAT097554	NONCODE	3.0822	up	chr4
19	NONHSAT071754	NONCODE	3.0350766	up	chr2
20	NONHSAT001268	NONCODE	3.0267425	up	chr1

Table 2
The top 20 downregulated lncRNA between RABV infected group and the Mock group.

Rank	Target ID	Database	Fold change	Regulation	Chromosomal Location
1	NONHSAT023581	NONCODE	4.8019395	down	chr11
2	NONHSAT081237	NONCODE	4.616764	down	chr21
3	NONHSAT121083	NONCODE	4.437275	down	chr7
4	NONHSAT067247	NONCODE	4.4165244	down	chr19
5	NONHSAT063914	NONCODE	3.4673083	down	chr19
6	ENST00000520314	Ensemble	3.3106384	down	chr12
7	NONHSAT006925	NONCODE	3.2039769	down	chr1
8	lnc-SOD1-10:1	LNCipedia	3.101424	down	chr21
9	NONHSAT115074	NONCODE	3.086726	down	chr6
10	NONHSAT063907	NONCODE	3.044938	down	chr19
11	NONHSAT139113	NONCODE	2.9804058	down	chrX
12	NONHSAT063916	NONCODE	2.9208074	down	chr19
13	NONHSAT089839	NONCODE	2.8861518	down	chr3
14	NONHSAT105227	NONCODE	2.7553966	down	chr5
15	NONHSAT055917	NONCODE	2.7237532	down	chr17
16	NONHSAT115533	NONCODE	2.7222123	down	chr6
17	NONHSAT023299	NONCODE	2.6433136	down	chr11
18	NONHSAT036297	NONCODE	2.6040115	down	chr14
19	ENST00000607804.1	Ensemble	2.583365	down	chr5
20	ENST00000596763	Ensemble	2.560574	down	chr19

Table 3
The top 20 differentially expressed mRNA between RABV infected group and the Mock group. Positive value and negative of fold change indicated upregulation and downregulation, respectively. *P*-value calculated from t-test and statistical significance was defined as $P < 0.05$.

Rank	GeneID	GeneSymbol	Fold change	Regulation
1	3303	HSPA1A	11.51535	Up
2	3304	HSPA1B	10.47574	Up
3	1958	EGR1	5.846022	Up
4	3434	IFIT1	5.074105	Up
5	51059	FAM135B	4.505088	Down
6	10673	TNFSF13B	4.424401	Up
7	79623	GALNT14	4.390206	Down
8	467	ATF3	3.994602	Up
9	10964	IFI44L	3.923585	Up
10	11013	TMSB15A	3.906712	Down
11	84618	NT5C1A	3.827048	Down
12	90102	PHLDB2	3.733078	Up
13	2246	FGF1	3.708205	Up
14	467	ATF3	3.496056	Up
15	1E+08	DNM1P35	3.437155	Down
16	4616	GADD45B	3.396232	Up
17	11174	ADAMTS6	3.39552	Up
18	57713	SFMBT2	3.273099	Down
19	2353	FOS	3.215419	Up
20	8935	SKAP2	3.146802	Up

used $TCID_{50}$ assays to generate a one-step growth curve for CVS-11 in SK-N-SH cells. As shown in Fig. 1B, virus titers gradually trended upward as the infection progressed, and at 24 hpi titers reached $10^{4.68}$ $TCID_{50}$/mL. Based on these results, we therefore selected the early stage of infection (under 24 h) for lncRNA and mRNA expression analysis in our microarray experiment

3.2. RABV infection alters the lncRNA and mRNA expression profile in SK-N-SH cells

To determine whether RABV infection affects expression of lncRNAs in human neuroblastoma cells, microarray analyses were performed to compare expression in CVS-11-infected and uninfected SK-N-SH cells. lncRNAs were classified as differentially expressed if they exhibited more than a 1.5-fold change in expression ($P < 0.05$). Among the differentially expressed lncRNAs, levels of 497 lncRNAs increased (i.e., levels were higher in infected cells), and 399 lncRNAs decreased (levels were lower in infected cells). The result of a hierarchical clustering analysis for all differentially expressed lncRNAs is shown in Fig. 2. The 20 lncRNAs exhibiting the most increased and decreased values are listed in Tables 1 and 2, respectively. Taken together, these results indicate that levels of individual lncRNAs are affected during RABV infection.

Because the microarray array includes 32,776 probes that can detect up to 13,664 mRNAs, we were able to identify differentially expressed

Table 4
Primers designed for quantitative real-time PCR.

Target ID	Forward primer (5'-3')	Reverse primer (5'-3')
TNFSF13B	GCGGGACTGAAAATCTTTGAAC	GCACTTCCCCTTTTAAAGCTG
IF144L	ACAGAGCCAAATGATTCCCTATG	TCGATAAACGACACACCAGTTG
EGR1	CAGCACCTTCAACCCTCAG	AGTCGAGTGGTTTGGCTG
GALNT14	CACTGCTGGTGTATTGCACG	CGGATCAGATGCGTAGGGG
TMSB15A	TCGGAAGTGGAGAAGTTTGAC	TCGAAATCTGCTGTTGGGAG
GAPDH	GCACCGTCAAGGCTGAGAAC	TGGTGAAGACGCCAGTGGA
NONHSAT130225	ACAATATCTGAGGAAAGAGCAGG	CTCATATCCTCTATTTGACCGCTC
NONHSAT078622	CTGTTCCCTCTTGGTTAGTCC	GTGGTAGTCTAGGCAATGGTG
NONHSAT013547	TTTGAGGAGGGAGGAGAGTG	GGGTAAGAGAAGGCAAGTAATG
ENST00000438538	GAATCTGGAACAGCGGTGGA	CGATGCCTTTGTCTTCTTGAGC
NRAV	GATGGTGCCGAATGTCTTCT	TGTTGCTCTTTCCGTTCCTT
LINC-PINT	GAACGAGGCAAGGAGCTAAA	AGCAAGGCAGAGAAACTCCA
NONHSAT063914	CTATTCAACGTCCTCCACCTC	TGCGACCTTGGCTCACTG
NR_126448	CACAGGAAAGATTGCGACTTC	TTCTGCTTCCCGAGTTCAAG
lnc-SOD1-10:1	ATTGGGTTGTGGCAAGCGGA	ACGAGTGATGGGGGAGGGGG

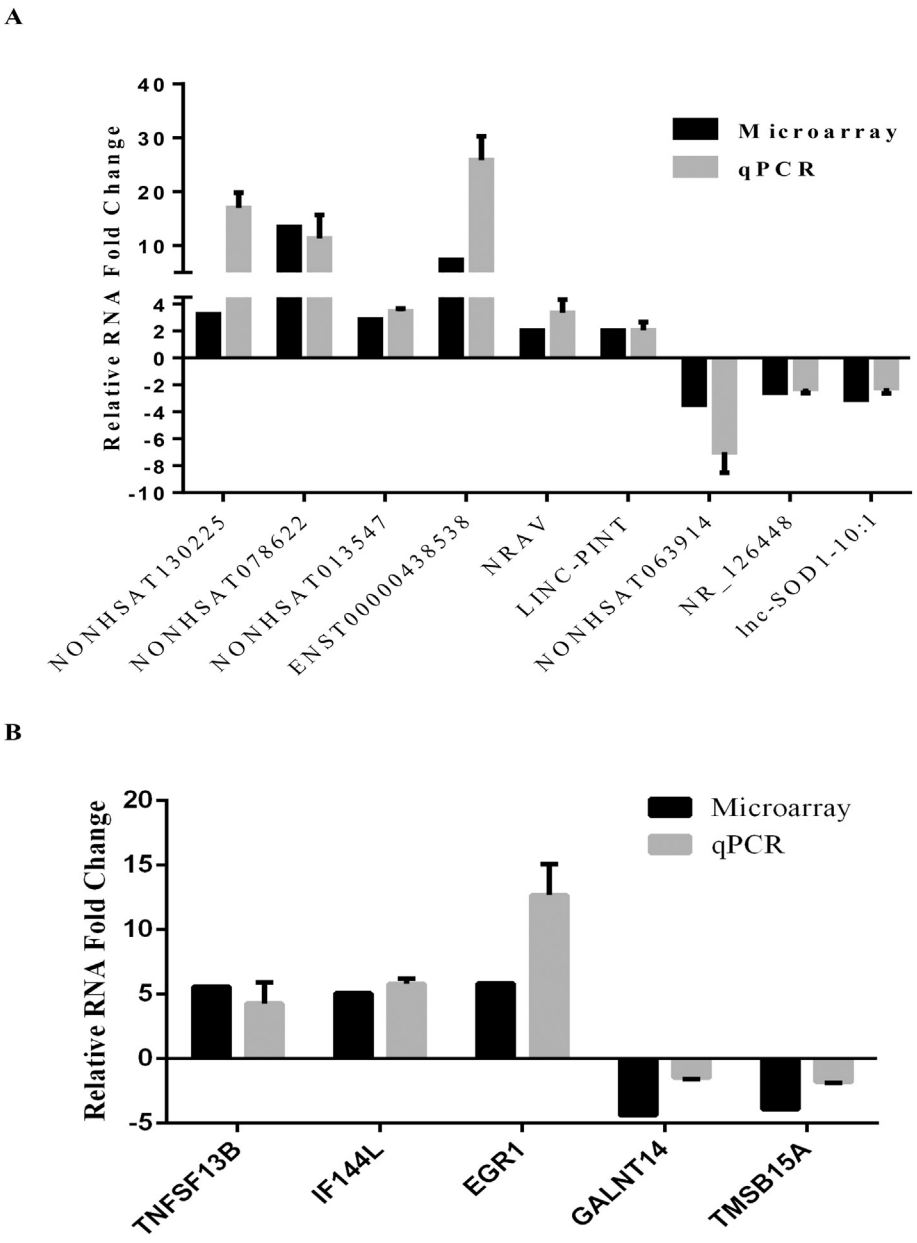

Fig. 3. Validation of microarray data using quantitative real-time PCR.

mRNAs (> 1.5-fold change; P < .05) in the same microarray experiment. 198 mRNAs decreased in abundance in RABV-infected cells, while 391 mRNAs exhibited increased levels. The 20 mRNAs exhibiting the largest fold changes are listed in Table 3.

3.3. Confirmation of RNA expression levels by qRT-PCR

To validate the expression levels determined using microarrays, 9 lncRNAs were selected for analysis by qRT-PCR (NONHSAT130225, NONHSAT078622, NONHSAT013547, ENST00000438538, NRAV, LINC-PINT, NONHSAT063914, NR_126448, and lnc-SOD1-10:1) along with 5 mRNAs (TNFSF13B, IF144L, EGR1, GALNT14, and TMSB15A). Specific primers (Table 4) were designed to amplify each target. The results showed that the lncRNAs and mRNAs had expression levels in RABV-infected cells consistent with those determined by microarray analysis (Fig. 3).

3.4. GO and KEGG pathway analyses of differentially expressed RNAs

Differentially expressed mRNAs were subjected to GO enrichment analysis to identify potential biological functions. Fig. 5 shows the results of the analysis for mRNAs that were down-regulated and up-regulated in RABV-infected SK-N-SH cells in biological process (BP) (Fig. 4). For mRNAs that increased in abundance, the top 3 enriched terms in the GO BP category were type I interferon signaling pathway, response to virus, and response to unfolded protein (Fig. 4A). For mRNAs that decreased in abundance, regulation of neuron migration (Fig. 4B), neuronal cell body (Fig. S1B), and core promoter binding (Fig. S2B) were the most enriched GO terms in the BP, cellular component(CC) and molecular function(MF) categories, respectively. The three most enriched terms in the CC category were focal adhesion, endoplasmic reticulum chaperone complex, and endocytic vesicle lumen (Fig. S1A). Finally, within the MF category, the top three terms were integrin binding, unfolded protein binding, and C3HC4-type RING finger domain binding (Fig. S2A).

To investigate biological pathways related to differentially

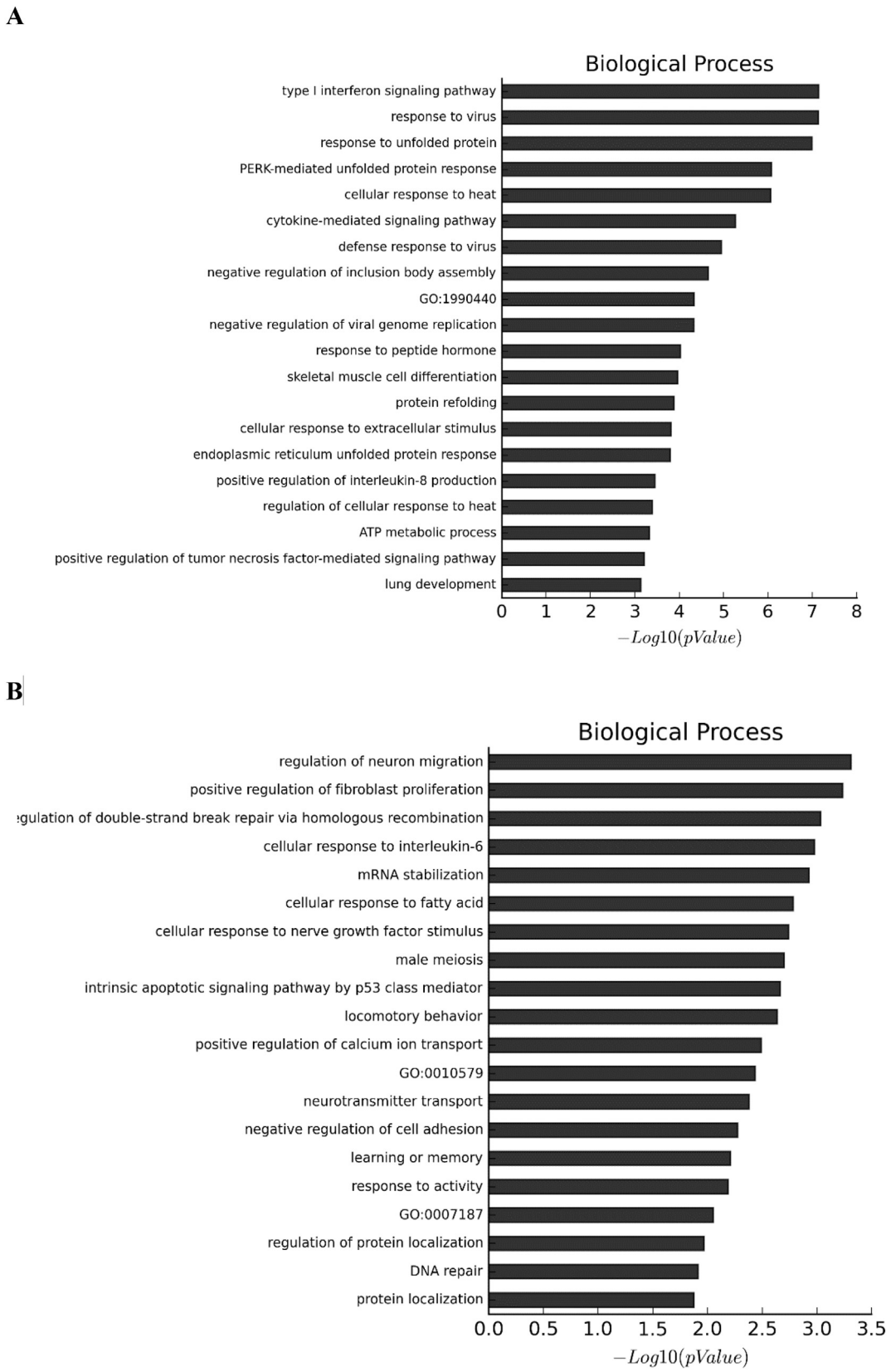

Fig. 4. GO analysis of differentially expressed mRNAs. GO terms for up-regulated (A) and down-regulated (B) genes, ranked by *P*-value. The statistical criteria in the analysis were P < .05 and FDR < 0.05. Only terms with the highest *P*-values are shown.

expressed mRNAs, KEGG Pathway analysis was performed. We found that the down-regulated mRNAs were associated with several enriched signaling pathways including “Protein processing in endoplasmic reticulum”, “Antigen processing and presentation”, “MAPK signaling pathway”, and “Pancreatic cancer” (Fig. 5A). The up-regulated mRNAs were associated with “Influenza A” and “Estrogen signaling pathway”

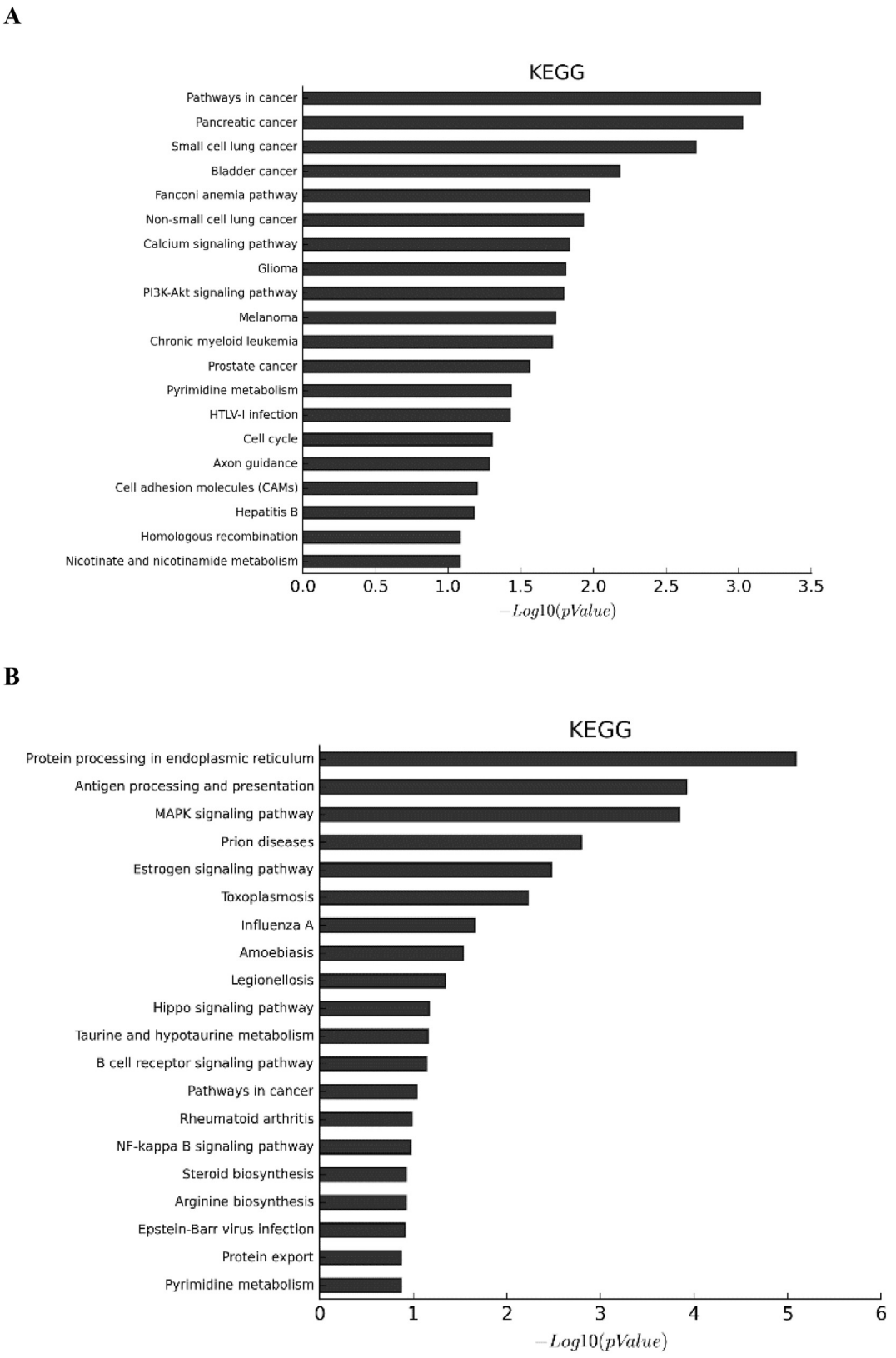

Fig. 5. KEGG pathway analysis of differentially expressed mRNAs. Pathways for upregulated genes (A) and downregulated genes (B), ranked by P-value. Only pathways with the highest P-values are shown.

(Fig.5B).

The results of the GO analysis and KEGG pathway analysis suggest that RABV infection regulates the interferon response, protein folding, and other signaling pathways.

3.5. lncRNA-mRNA co-expression analysis and prediction of lncRNA function

896 lncRNAs were co-expressed with 579 mRNAs. In order to

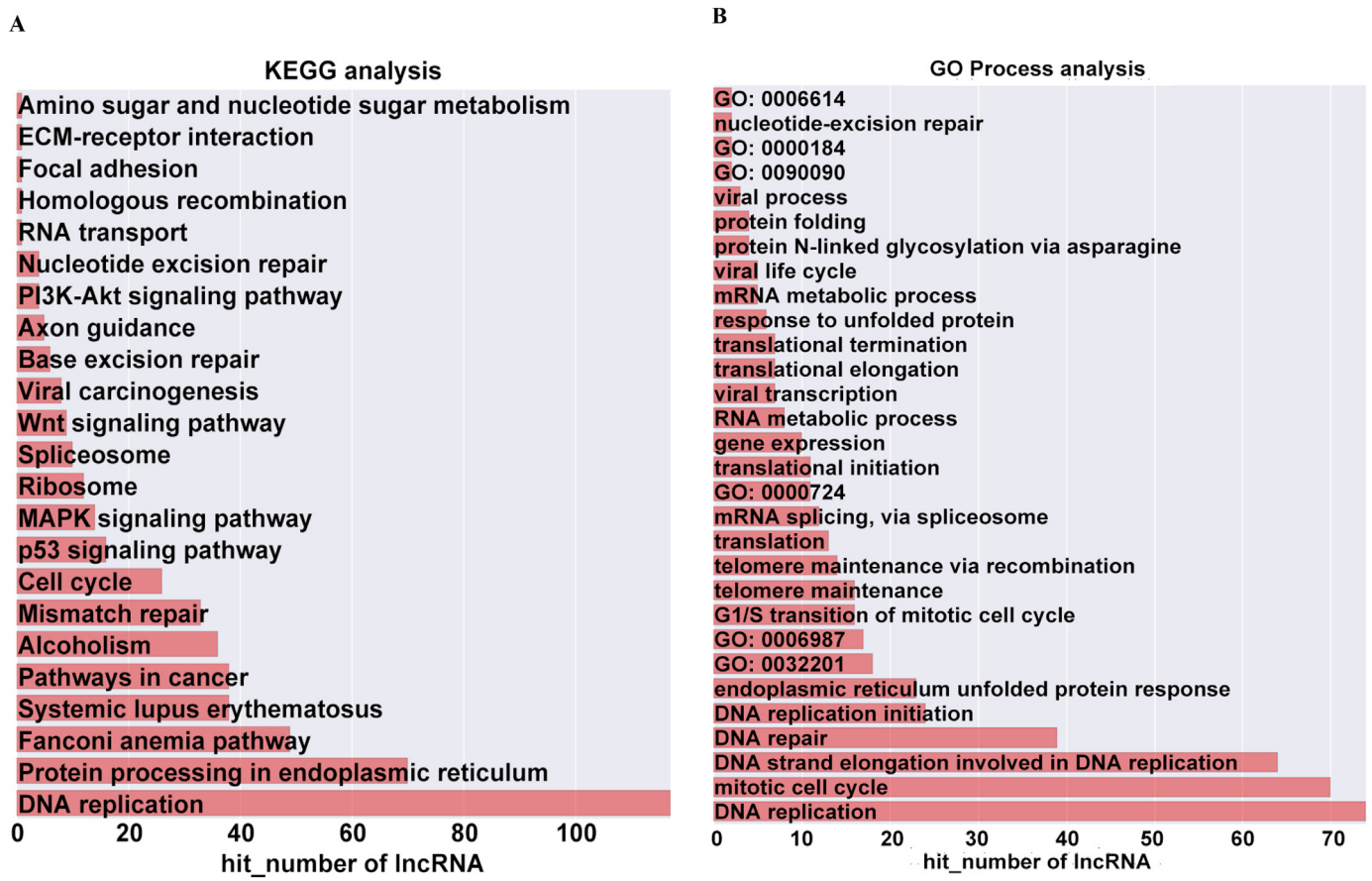

Fig. 6. Functional predictions for lncRNAs. (A) LncRNA functions inferred using KEGG pathways. The x-coordinate shows the number of unique LncRNAs enriched in each pathway. ID and description are shown on the y-axis. (B) LncRNA functions inferred using GO process terms. The x-coordinate shows the number of unique LncRNAs enriched in each ID and description are shown on the y-axis.

explore the correlation between them, we constructed a lncRNA-mRNA co-expression network based on a correlation analysis. The complete results are listed in (Supplemental Table 1). LncRNA functions were predicted using the KEGG pathway annotations and GO terms for the co-expressed mRNAs. To reflect the overall situation of the difference in the distribution of lncRNAs function in the experiment, we select the reliability prediction terms (according to the *P*-value and enrichment). As shown in Fig. 6A, 117 lncRNAs clustered into the DNA repair pathway. All KEGG enrichment results are listed in (Supplemental Table 2). 74 lncRNAs clustered into DNA replication in the GO Process category (Fig.6B). All GO enrichment results are listed in (Supplemental Table 3).

3.6. Cis-regulation of lncRNAs

To explore whether lncRNAs might function as cis-regulatory factors, we examined their co-expressed mRNAs to determine whether the respective lncRNA- and mRNA-encoding genes were in close proximity (100 kbp). 28 lncRNAs were predicted to participate cis-regulation (Table 5). One of the potential cis targets, Hsp90, is associated with cellular processes during RABV infection. We recently reported that RABV infection increase expression of Hsp90, and Hsp90 maintains viral P protein stability by preventing protein degradation (Xu et al., 2016). The functions of the other candidate cis gene targets have not been determined.

3.7. Trans-regulation of lncRNAs

When examining lncRNA function, “trans” regulatory mechanisms that affect chromatin, transcription, or other processes must be considered (Bassett et al., 2014). As a step in this direction, co-expressed lncRNA-mRNA pairs were examined to identify mRNAs that encode known transcription factors. A complete list of TF-lncRNA pairs is shown in Supplemental Table 4. Because the number of TF-lncRNA pairs is so large (> 3700), it is not practical to generate a network directly from this data. To simplify the network, we selected the top 100 pairs (ranked by P-value; see Supplemental Table 5) to generate a core network map (shown in Fig. 7A). Most of the predicted trans-regulatory lncRNAs participate in pathways regulated by the TFs E2F4, TAF7, KAT2A, TBP, POU2F2, and BCLAF1. The top 100 co-expressed gene pairs were also used to construct a lncRNA-TF-mRNA network (see Supplemental Table 6). The network structure, shown in Fig. 8B, suggests that the TFs E2F4, and TAF7, along with ten lncRNAs are transcriptional regulators that play important roles in various signal pathways (Fig. 7B).

4. Discussion

Although gene and protein expression has been extensively studied in cells infected by RABV, it is not clear how host regulatory mechanisms affect RABV replication and infection. However, growing evidence suggests that lncRNAs are involved in the virus life cycle and may modulate viral infection. For example, in response to infection by vesicular stomatitis virus, lncRNA-ACOD1 is induced (Wang et al., 2017b). The same lncRNA appears after infection by Sendai virus, vaccinia virus, and herpes simplex virus type 1. lncRNA-ACOD1 directly binds glutamic-oxaloacetic transaminase (GOT2) near the substrate niche, enhancing its catalytic activity and thereby promoting viral

Table 5
"Cis" genes of aberrant lncRNAs.

lncRNA ID	mRNA gene symbol	*p*-value	Pearson correlation	cis_distance
ENST00000520314	LOC102724747	0.0015	0.968	2251
NR_045612	ZNF391	0.022	0.877	75945
lnc_AIF1_3_7	LST1	0.005	0.942	48314
lnc_AIF1_3_7	TNF	0.034	0.846	58850
lnc_AIF1_3_7	LY6G5B	0.021	0.878	34839
lnc_ANXA1_5_1	ANXA1	0.01	0.917	1270
lnc_AP2A1_1_1	CPT1C	0.0028	0.956	96296
lnc_C5orf47_4_1	HMP19	0.00024	0.987	44322
lnc_CETP_1_2	HERPUD1	0.0017	0.966	2503
lnc_CETP_3_1	HERPUD1	0.0013	0.97	1684
lnc_CYB561D2_3_1	LSMEM2	0.0075	0.929	78547
lnc_DBF4_2_1	ADAM22	0.0027	0.957	20438
lnc_FRY_1_1	FRY	0.049	0.814	43838
lnc_GABPA_10_1	JAM2	0.0047	0.944	73320
lnc_GLI2_6_1	GLI2	0.04	0.831	40363
lnc_HIST1H4A_1_1	HIST1H4C	0.005	0.941	60130
lnc_HIST1H4A_1_1	HIST1H3A	0.015	0.899	23339
lnc_HIST1H4A_1_1	HIST1H4A	0.024	0.871	22039
lnc_LLGL2_3_5	TSEN54	0.0094	0.92	82553
lnc_MYO18B_3_2	ADRBK2	0.00046	0.982	84326
lnc_PDCD1LG2_3_2	PDCD1LG2	0.0015	0.968	94542
lnc_PDCD1LG2_3_2	CD274	0.00031	0.986	5160
lnc_PDE7B_5_1	MYB	7.90E-05	0.993	15198
lnc_PEAR1_1_1	NTRK1	0.031	0.853	56082
lnc_PFKM_1_4	TMEM106C	0.03	0.854	3210
lnc_PHOSPHO2_1_1	PHOSPHO2_KLHL23	0.016	0.894	8149
lnc_PLEKHG1_2_1	MTHFD1L	0.031	0.854	82663
lnc_PPIA_4_2	ZMIZ2	0.04	0.833	3738
lnc_RP11_366K18.3.1_1_1	TRIM55	0.0064	0.934	2930
lnc_RP11_366K18.3.1_2_1	TRIM55	0.0049	0.942	22584
lnc_TDG_2_1	HSP90B1	0.047	0.818	15637
lnc_TMEM132A_1_2	ZP1	0.025	0.868	49892
lnc_TMEM132A_1_2	TMEM132A	0.016	0.894	11445
lnc_TMEM184C_1_1	EDNRA	0.00012	0.991	37911

infection (Wang et al., 2017b). The lncRNA NEAT1 inhibits HIV replication by suppressing the export of Rev-dependent instability element (INS)-containing HIV-1 mRNAs from the nucleus to the cytoplasm (Zhang et al., 2013a). NEAT1 also modulates the innate immune response against Hantaan virus infection by acting as a positive feedback for RIG-I signaling (Ma et al., 2017). LncRNA-BISPR is up-regulated in response to IFN in different cell lines, and regulates the expression of the antiviral factor BST2 (Barriocanal et al., 2015). Finally, lincRNA-COX2, lncRNA-NRAV, NEAT1, and other lncRNAs are involved in the regulation of the immune response (Imamura et al., 2014; Carpenter et al., 2013; Kambara et al., 2014; Ouyang et al., 2014).

Here, we report the first evidence that RABV infection regulates the expression of lncRNAs in the human neuroblastoma cell line SK-N-SH, widely used in studying the host response to RABV. We found that 896 lncRNA and 579 mRNA transcripts are differentially expressed. Because many lncRNAs have been identified as modulators in virus-induced host immune and inflammatory responses, we predict that these lncRNAs play crucial roles in regulating the immune response to RABV, although understanding the mechanisms by which they exert their effects will require further exploration.

Interestingly, we found that NRAV, a lncRNA that is markedly down-regulated during infection with influenza A virus (IAV) and several other viruses (Ouyang et al., 2014), is up-regulated in response to RABV (Fig.4A). NRAV is also up-regulated in HuH7 cells after infection by Ebola virus and Marburg virus (Holzer et al., 2016). The discrepancies in these expression patterns may be due to host cell and virus differences. Since NRAV plays a key role in regulating antiviral innate immunity via the suppression of interferon-stimulated gene transcription during IAV infection (Ouyang et al., 2014), it is possible that it affects RABV proliferation. We also observed that lncRNA lnc-KLF14–2:4, which has been designated Linc-PINT by other investigators, is up-regulated in RABV-infected SK-N-SH cells. Linc-PINT is regulated by p53 and inhibits tumor cell invasion by reducing the invasive phenotype of cancer cells (Marin-Bejar et al., 2017; Marin-Bejar et al., 2013). It is therefore another promising candidate for future investigation.

To explore the potential functions of lncRNAs, GO term enrichment and KEGG pathway analyses were conducted to characterize the co-expressed mRNAs. The up-regulated lncRNAs were significantly associated with type I interferon signaling, response to virus, and response to unfolded protein. These results are consistent with reports that interferon-stimulated genes are also stimulated in RABV-infected BV2 cells (Zhao et al., 2013). The most enriched pathways for the up-regulated lncRNAs included protein processing in endoplasmic reticulum, antigen processing and presentation, and MAPK signaling pathway. We reported previously that the MAPK signaling pathway is involved in CASP2-dependent autophagy during RABV infection (Liu et al., 2017). In contrast, the GO terms core promoter binding, neuronal cell body, and regulation of neuron migration were enriched for the down-regulated lncRNAs. Intriguingly, upregulated mRNAs show enrichment in many cancer-related pathways, meaning that these genes, as previously reported tumor-related genes, may play a role in immune and inflammatory responses (Munoz-Fontela et al., 2016).

The co-expression relationships were obtained by network construction based on differentially expressed mRNAs and differentially expressed lncRNAs in RABV infection (Supplemental Table 1). Among these co-expressed relationships, we found that the given lncRNA can be co-expressed with many mRNAs, suggesting that a lncRNA may be regulated by many mRNAs. And, functional prediction based on co-expression analysis provided valuable resources for lncRNA research (Supplemental Table 2 & Supplemental Table 3). Taking an example of lncRNA_NR_038854, known as NRAV, we firstly calculated co-

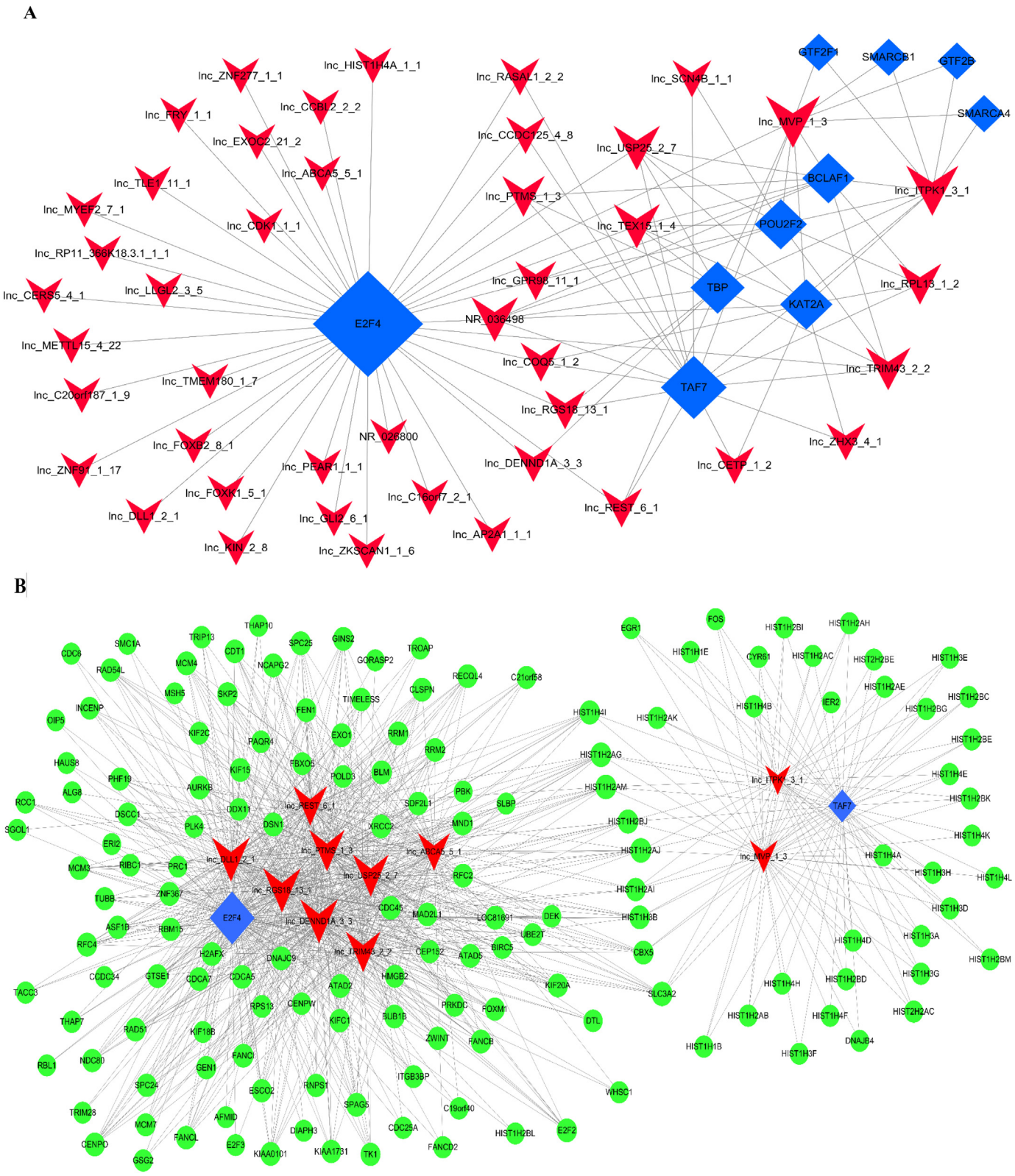

Fig. 7. Co-expression network consisting of lncRNAs, mRNAs and transcription factors (TFs). (A) lncRNA-TF network. Blue nodes are transcription factors, and the red nodes are LncRNAs. Node size is proportional to the number of connected edges. (B) lncRNA-mRNA-TF network. Blue nodes are transcription factors, and red nodes are LncRNAs. Target genes are represented by green nodes. Node size is directly proportional to the number of connected edges. The relationship between the thickness and the statistical result is proportional to the number of times. (For interpretation of the references to colour in this figure legend, the reader is referred to the web version of this article.)

expressed mRNAs for lncRNA_NR_038854, and then we conduct a functional enrichment analysis of this set of co-expressed mRNAs. The enriched functional terms of KEGG including: Influenza A, MAPK signaling pathway, Protein processing in endoplasmic reticulum, and so on. This result was consistent with previous report (Ouyang et al., 2014). However, the correlations between expression of lncRNAs and mRNAs are based on replicates of only two conditions and need more data points for future validation.

Functions for putative trans-regulatory lncRNAs were inferred from the TFs that were co-expressed with them. The structure of the core regulatory network suggests that the lncRNAs are regulated by E2F4 and TAF7. E2F4 (an E2F TF family member) is probably a repressor of transcription. The many E2F4 targets in the genome potentially regulate the cell cycle, DNA damage repair, apoptosis, mRNA processing, and ubiquitination. lncRNA-GAS5 promotes bladder cancer cell apoptosis by interacting with E2F4 and recruiting E2F4 to the EZH2 promoter, thereby directly inhibiting EZH2 transcription (Wang et al., 2018). Additional research will be necessary to determine how E2F4 and its associated lncRNAs are involved in pathogenesis of RABV infection. As part of the TFIID complex, TAF7 helps to recruit RNA polymerase II and other factors to class II promoters, and is necessary for transcription from these promoters (Gegonne et al., 2008). Expression of TAF7-dependent mRNAs is greatly diminished during poliovirus infection, and TAF7 controls the transcription of a series of interferon-induced proteins such as IFIT1, IFIT2, and ISG15 (Doukas and Sarnow, 2011).

In conclusion, differentially expressed lncRNAs were identified in RABV-infected SK-N-SH cells. lncRNA functions were tentatively assigned using annotations associated with the co-expressed mRNAs, using GO, KEGG, and other sources. Despite the fact that only a limited number of differentially expressed lncRNAs could be characterized using this method, the results help to illuminate RABV pathogenesis and the host response. Additional studies will be necessary to confirm the roles played by these lncRNAs, and may lead to novel approaches for preventing and treating rabies.

Author contributions

Design and supervise the study: JYZ and SS. Perform the experiments: SLJ, MYZ, JYZ, YCC, XFZ, DW and GRL. Prepare the manuscript: SLJ, SS and JYZ.

Measurements for (A) nine selected lncRNAs and (B) five selected mRNAs.

Acknowledgements

This work was funded by the National Key Research and Development Program of China (2016YFD0500402), National Natural Science Foundation of China (31802195), the Natural Science Foundation of Jiangsu Province (BK20170721), China Association for science and technology youth talent lift project and the Fundamental Research Funds for the Central Universities (Y0201600147).

Appendix A. Supplementary data

Supplementary data to this article can be found online at https://doi.org/10.1016/j.meegid.2018.10.027.

References

Barriocanal, M., Camero, E., Segura, V., Fortes, P., 2015. Long non-coding RNA BST2/BISPR is induced by IFN and regulates the expression of the antiviral factor tetherin. Front. Immunol. 5, 1–13.

Bassett, A.R., Akhtar, A., Barlow, D.P., Bird, A.P., Brockdorff, N., Duboule, D., Ephrussi, A., Ferguson-Smith, A.C., Gingeras, T.R., Haerty, W., Higgs, D.R., Miska, E.A., Ponting, C.P., 2014. Considerations when investigating lncRNA function in vivo. elife 3.

Carpenter, S., Aiello, D., Atianand, M.K., Ricci, E.P., Gandhi, P., Hall, L.L., Byron, M., Monks, B., Henry-Bezy, M., Lawrence, J.B., O'Neill, L.A.J., Moore, M.J., Caffrey, D.R., Fitzgerald, K.A., 2013. A long noncoding RNA mediates both activation and repression of immune response genes. Science 341 (6147), 789–792.

Chen, X., Yan, G.Y., 2013. Novel human lncRNA-disease association inference based on lncRNA expression profiles. Bioinformatics 29 (20), 2617–2624.

Derrien, T., Johnson, R., Bussotti, G., Tanzer, A., Djebali, S., Tilgner, H., Guernec, G., Martin, D., Merkel, A., Knowles, D.G., Lagarde, J., Veeravalli, L., Ruan, X.A., Ruan, Y.J., Lassmann, T., Carninci, P., Brown, J.B., Lipovich, L., Gonzalez, J.M., Thomas, M., Davis, C.A., Shiekhattar, R., Gingeras, T.R., Hubbard, T.J., Notredame, C., Harrow, J., Guigo, R., 2012. The GENCODE v7 catalog of human long noncoding RNAs: Analysis of their gene structure, evolution, and expression. Genome Res. 22 (9), 1775–1789.

Djebali, S., Davis, C.A., Merkel, A., Dobin, A., Lassmann, T., Mortazavi, A., Tanzer, A., Lagarde, J., Lin, W., Schlesinger, F., Xue, C.H., Marinov, G.K., Khatun, J., Williams, B.A., Zaleski, C., Rozowsky, J., Roder, M., Kokocinski, F., Abdelhamid, R.F., Alioto, T., Antoshechkin, I., Baer, M.T., Bar, N.S., Batut, P., Bell, K., Bell, I., Chakrabortty, S., Chen, X., Chrast, J., Curado, J., Derrien, T., Drenkow, J., Dumais, E., Dumais, J., Duttagupta, R., Falconnet, E., Fastuca, M., Fejes-Toth, K., Ferreira, P., Foissac, S., Fullwood, M.J., Gao, H., Gonzalez, D., Gordon, A., Gunawardena, H., Howald, C., Jha, S., Johnson, R., Kapranov, P., King, B., Kingswood, C., Luo, O.J., Park, E., Persaud, K., Preall, J.B., Ribeca, P., Risk, B., Robyr, D., Sammeth, M., Schaffer, L., See, L.H., Shahab, A., Skancke, J., Suzuki, A.M., Takahashi, H., Tilgner, H., Trout, D., Walters, N., Wang, H., Wrobel, J., Yu, Y.B., Ruan, X.A., Hayashizaki, Y., Harrow, J., Gerstein, M., Hubbard, T., Reymond, A., Antonarakis, S.E., Hannon, G., Giddings, M.C., Ruan, Y.J., Wold, B., Carninci, P., Guigo, R., Gingeras, T.R., 2012. Landscape of transcription in human cells. Nature 489 (7414), 101–108.

Doukas, T., Sarnow, P., 2011. Escape from transcriptional shutoff during poliovirus infection: NF-kappa B-Responsive Genes I kappa Ba and A20. J. Virol. 85 (19), 10101–10108.

Fatica, A., Bozzoni, I., 2014. Long non-coding RNAs: new players in cell differentiation and development. Nat Rev Genet 15 (1), 7–21.

Fu, Z.F., 1997. Rabies and rabies-research: past, present and future. Vaccine 15, S20–S24.

Gegonne, A., Weissman, J.D., Lu, H.X., Zhou, M.S., Dasguptat, A., Ribble, R., Brady, J.N., Singer, D.S., 2008. TFIID component TAF7 functionally interacts with both TFIIH and P-TEFb. P Natl Acad Sci USA 105 (14), 5367–5372.

Gendrel, A.V., Heard, E., 2014. Noncoding RNAs and Epigenetic Mechanisms during X-Chromosome Inactivation. Annu Rev Cell Dev Bi 30, 561–580.

Guenzl, P.M., Barlow, D.P., 2012. Macro lncRNAs. A new layer of cis-regulatory information in the mammalian genome. Rna Biol 9 (6), 731–741.

Guttman, M., Amit, I., Garber, M., French, C., Lin, M.F., Feldser, D., Huarte, M., Zuk, O., Carey, B.W., Cassady, J.P., Cabili, M.N., Jaenisch, R., Mikkelsen, T.S., Jacks, T., Hacohen, N., Bernstein, B.E., Kellis, M., Regev, A., Rinn, J.L., Lander, E.S., 2009. Chromatin signature reveals over a thousand highly conserved large non-coding RNAs in mammals. Nature 458 (7235), 223–227.

Holzer, M., Krahling, V., Amman, F., Barth, E., Bernhart, S.H., Carmelo, V.A.O., Collatz, M., Doose, G., Eggenhofer, F., Ewald, J., Fallmann, J., Feldhahn, L.M., Fricke, M., Gebauer, J., Gruber, A.J., Hufsky, F., Indrischek, H., Kanton, S., Linde, J., Mostajo, N., Ochsenreiter, R., Riege, K., Rivarola-Duarte, L., Sahyoun, A.H., Saunders, S.J., Seemann, S.E., Tanzer, A., Vogel, B., Wehner, S., Wolfinger, M.T., Backofen, R., Gorodkin, J., Grosse, I., Hofacker, I., Hoffmann, S., Kaleta, C., Stadler, P.F., Becker, S., Marz, M., 2016. Differential transcriptional responses to Ebola and Marburg virus infection in bat and human cells. Sci. Rep.-Uk 6.

Hu, B.X., Huo, Y.X., Yang, L.P., Chen, G.J., Luo, M.H., Yang, J.L., Zhou, J.M., 2017. ZIKV infection effects changes in gene splicing, isoform composition and lncRNA expression in human neural progenitor cells. Virol. J. 14.

Huang, J., Zhou, N., Watabe, K., Lu, Z., Wu, F., Xu, M., Mo, Y.Y., 2014. Long non-coding RNA UCA1 promotes breast tumor growth by suppression of p27 (Kip1). Cell Death Dis. 5.

Imamura, K., Imamachi, N., Akizuki, G., Kumakura, M., Kawaguchi, A., Nagata, K., Kato, A., Kawaguchi, Y., Sato, H., Yoneda, M., Kai, C., Yada, T., Suzuki, Y., Yamada, T., Ozawa, T., Kaneki, K., Inoue, T., Kobayashi, M., Kodama, T., Wada, Y., Sekimizu, K., Akimitsu, N., 2014. Long noncoding RNA NEAT1-dependent SFPQ relocation from promoter region to paraspeckle mediates IL8 expression upon immune stimuli. Mol. Cell 53 (3), 393–406.

Kambara, H., Niazi, F., Kostadinova, L., Moonka, D.K., Siegel, C.T., Post, A.B., Carnero, E., Barriocanal, M., Fortes, P., Anthony, D.D., Valadkhan, S., 2014. Negative regulation of the interferon response by an interferon-induced long non-coding RNA. Nucleic Acids Res. 42 (16), 10668–U805.

Kretz, M., Siprashvili, Z., Chu, C., Webster, D.E., Zehnder, A., Qu, K., Lee, C.S., Flockhart, R.J., Groff, A.F., Chow, J., Johnston, D., Kim, G.E., Spitale, R.C., Flynn, R.A., Zheng, G.X.Y., Aiyer, S., Raj, A., Rinn, J.L., Chang, H.Y., Khavari, P.A., 2013. Control of somatic tissue differentiation by the long non-coding RNA TINCR. Nature 493 (7431), 231–U245.

Lee, J.T., 2012. Epigenetic regulation by long noncoding RNAs. Science 338 (6113), 1435–1439.

Li, Z.H., Rana, T.M., 2014. Decoding the noncoding: prospective of lncRNA-mediated innate immune regulation. RNA Biol. 11 (8), 979–985.

Li, Y.C., Zhang, H., Zhu, B.B., Ashraf, U., Chen, Z., Xu, Q.P., Zhou, D.Y., Zheng, B.H., Song, Y.F., Chen, H.C., Ye, J., Cao, S.B., 2017. Microarray Analysis Identifies the potential Role of Long Non-Coding RNA in regulating neuroinflammation during Japanese encephalitis virus infection. Front. Immunol. 8.

Liu, J., Wang, H.L., Gu, J.Y., Deng, T.J., Yuan, Z.C., Hu, B.L., Xu, Y.B., Yan, Y., Zan, J., Liao, M., Dicaprio, E., Li, J.R., Su, S., Zhou, J.Y., 2017. BECN1-dependent CASP2 incomplete autophagy induction by binding to rabies virus phosphoprotein. Autophagy 13 (4), 739–753.

Lu, K.H., Li, W., Liu, X.H., Sun, M., Zhang, M.L., Wu, W.Q., Xie, W.P., Hou, Y.Y., 2013. Long non-coding RNA MEG3 inhibits NSCLC cells proliferation and induces apoptosis by affecting p53 expression. BMC Cancer 13.

Luo, Z.H., Li, Y., Liu, X.F., Luo, M.C., Xu, L.Q., Luo, Y.B., Xiao, B., Yang, H., 2015. Systems biology of myasthenia gravis, integration of aberrant lncRNA and mRNA expression changes. BMC Med. Genet. 8.

Ma, H.W., Han, P.J., Ye, W., Chen, H.S., Zheng, X.Y., Cheng, L.F., Zhang, L., Yu, L., Wu, X.G., Xu, Z.K., Lei, Y.F., Zhang, F.L., 2017. The Long Noncoding RNA NEAT1 Exerts Antihantaviral Effects by acting as positive Feedback for RIG-I Signaling. J. Virol. 91 (9).

Marin-Bejar, O., Marchese, F.P., Athie, A., Sanchez, Y., Gonzalez, J., Segura, V., Huang, L.L., Moreno, I., Navarro, A., Monzo, M., Garcia-Foncillas, J., Rinn, J.L., Guo, S.L., Huarte, M., 2013. Pint lincRNA connects the p53 pathway with epigenetic silencing by the Polycomb repressive complex 2. Genome Biol. 14 (9).

Marin-Bejar, O., Mas, A.M., Gonzalez, J., Martinez, D., Athie, A., Morales, X., Galduroz, M., Raimondi, I., Grossi, E., Guo, S.L., Rouzaut, A., Ulitsky, I., Huarte, M., 2017. The human lncRNA LINC-PINT inhibits tumor cell invasion through a highly conserved sequence element. Genome Biol. 18.

Munoz-Fontela, C., Mandinova, A., Aaronson, S.A., Lee, S.W., 2016. Emerging roles of p53 and other tumour-suppressor genes in immune regulation. Nat Rev Immunol 16 (12), 741–750.

Ouyang, J., Zhu, X.M., Chen, Y.H., Wei, H.T., Chen, Q.H., Chi, X.J., Qi, B.M., Zhang, L.F., Zhao, Y., Gao, G.F., Wang, G.S., Chen, J.L., 2014. NRAV, a Long Noncoding RNA, Modulates Antiviral responses through suppression of Interferon-Stimulated Gene Transcription. Cell Host Microbe 16 (5), 616–626.

Pandey, A.D., Goswami, S., Shukla, S., Das, S., Ghosal, S., Pal, M., Bandyopadhyay, B., Ramachandran, V., Basu, N., Sood, V., Pandey, P., Chakrabarti, J., Vrati, S., Banerjee, A., 2017. Correlation of altered expression of a long non-coding RNA, NEAT1, in peripheral blood mononuclear cells with dengue disease progression. J. Inf. Secur. 75 (6), 541–554.

Saha, S., Murthy, S., Rangarajan, P.N., 2006. Identification and characterization of a virus-inducible non-coding RNA in mouse brain. J Gen Virol 87 1991-1995.

Sauvageau, M., Goff, L.A., Lodato, S., Bonev, B., Groff, A.F., Gerhardinger, C., Sanchez-Gomez, D.B., Hacisuleyman, E., Li, E., Spence, M., Liapis, S.C., Mallard, W., Morse, M., Swerdel, M.R., D'Ecclessis, M.F., Moore, J.C., Lai, V., Gong, G.C., Yancopoulos, G.D., Frendewey, D., Kellis, M., Hart, R.P., Valenzuela, D.M., Arlotta, P., Rinn, J.L., 2013. Multiple knockout mouse models reveal lincRNAs are required for life and brain development. elife 2.

Storey, J.D., 2002. A direct approach to false discovery rates. J Roy Stat Soc B 64, 479–498.

Sun, W.C., Pei, L., Liang, Z.D., 2017. mRNA and Long Non-coding RNA Expression Profiles in Rats Reveal Inflammatory Features in Sepsis-Associated Encephalopathy. Neurochem. Res. 42 (11), 3199–3219.

Tan, J.M., Wang, R.Y., Ji, S.L., Su, S., Zhou, J.Y., 2017. One Health strategies for rabies control in rural areas of China. Lancet Infect. Dis. 17 (4), 365–367.

Wang, P., Xue, Y.Q., Han, Y.M., Lin, L., Wu, C., Xu, S., Jiang, Z.P., Xu, J.F., Liu, Q.Y., Cao, X.T., 2014. The STAT3-Binding Long Noncoding RNA lnc-DC Controls Human Dendritic Cell Differentiation. Science 344 (6181), 310–313.

Wang, K., Liu, C.Y., Zhou, L.Y., Wang, J.X., Wang, M., Zhao, B., Zhao, W.K., Xu, S.J., Fan, L.H., Zhang, X.J., Feng, C., Wang, C.Q., Zhao, Y.F., Li, P.F., 2015. APF lncRNA regulates autophagy and myocardial infarction by targeting miR-188-3p. Nat. Commun. 6.

Wang, J.Y., Ma, R.X., Ma, W., Chen, J., Yang, J.C., Xi, Y.G., Cui, Q.H., 2016. LncDisease: a sequence based bioinformatics tool for predicting lncRNA-disease associations. Nucleic Acids Res. 44 (9).

Wang, Z.Q., Fan, P., Zhao, Y.W., Zhang, S.K., Lu, J.H., Xie, W.D., Jiang, Y.Y., Lei, F., Xu, N.H., Zhang, Y., 2017a. NEAT1 modulates herpes simplex virus-1 replication by regulating viral gene transcription. Cell. Mol. Life Sci. 74 (6), 1117–1131.

Wang, P., Xu, J.F., Wang, Y.J., Cao, X.T., 2017b. An interferon-independent lncRNA promotes viral replication by modulating cellular metabolism. Science 358 (6366), 1051–1055.

Wang, M., Guo, C., Wang, L., Luo, G., Huang, C., Li, Y., Liu, D., Zeng, F., Jiang, G., Xiao, X., 2018. Long noncoding RNA GAS5 promotes bladder cancer cells apoptosis through inhibiting EZH2 transcription. Cell Death Dis. 9 (2), 238.

Welburn, S.C., Beange, I., Ducrotoy, M.J., Okello, A.L., 2015. The neglected zoonoses-the case for integrated control and advocacy. Clin Microbiol Infec 21 (5), 433–443.

Wu, G.Z., Cai, J., Han, Y., Chen, J.H., Huang, Z.P., Chen, C.Y., Cai, Y., Huang, H.F., Yang, Y.J., Liu, Y.K., Xu, Z.C., He, D.F., Zhang, X.Q., Hu, X.Y., Pinello, L., Zhong, D., He, F.T., Yuan, G.C., Wang, D.Z., Zeng, C.Y., 2014. LincRNA-p21 regulates neointima formation, vascular smooth muscle cell proliferation, apoptosis, and atherosclerosis by enhancing p53 activity. Circulation 130 (17), 1452–U64.

Wu, J., Li, S., Zheng, Y., Zhang, M.M., Zhang, H.L., Sun, Y., Yu, B., 2017. Silencing of lncRNA NEAT1 induces tolerogenic dendritic cells and immune tolerance in heart transplantation. J. Immunol. 198 (1).

Xiong, H., Ni, Z., He, J., Jiang, S., Li, X., He, J., Gong, W., Zheng, L., Chen, S., Li, B., Zhang, N., Lyu, X., Huang, G., Chen, B., Zhang, Y., He, F., 2017. LncRNA HULC triggers autophagy via stabilizing Sirt1 and attenuates the chemosensitivity of HCC cells. Oncogene 36 (25), 3528–3540.

Xu, Y.B., Liu, F., Liu, J., Wang, D.D., Yan, Y., Ji, S.L., Zan, J., Zhou, J.Y., 2016. The co-chaperone Cdc37 regulates the rabies virus phosphoprotein stability by targeting to Hsp90AA1 machinery. Sci. Rep.-Uk 6.

Yang, X.F., Yang, J.H., Wang, J.L., Wen, Q., Wang, H., He, J.C., Hu, S.F., He, W.T., Du, X.L., Liu, S.D., Ma, L., 2016. Microarray analysis of long noncoding RNA and mRNA expression profiles in human macrophages infected with Mycobacterium tuberculosis. Sci Rep-Uk 6.

Zhang, Q., Chen, C.Y., Yedavalli, V.S.R.K., Jeang, K.T., 2013a. NEAT1 Long Noncoding RNA and paraspeckle bodies modulate HIV-1 posttranscriptional expression. MBio 4 (1).

Zhang, J.Y., Wu, X.P., Zan, J., Wu, Y.P., Ye, C.J., Ruan, X.Z., Zhou, J.Y., 2013b. Cellular chaperonin CCT gamma contributes to rabies virus replication during infection. J. Virol. 87 (13), 7608–7621.

Zhao, P.S., Yang, Y.J., Feng, H., Zhao, L.L., Qin, J.L., Zhang, T., Wang, H.L., Yang, S.T., Xia, X.Z., 2013. Global gene expression changes in BV2 microglial cell line during rabies virus infection. Infect. Genet. Evol. 20, 257–269.